Since January 2020 Elsevier has created a COVID-19 resource centre with free information in English and Mandarin on the novel coronavirus COVID-19. The COVID-19 resource centre is hosted on Elsevier Connect, the company's public news and information website.

Biosensors and Bioelectronics 195 (2022) 113647

Contents lists available at ScienceDirect

Biosensors and Bioelectronics

journal homepage: www.elsevier.com/locate/bios

Highly sensitive and ultra-rapid antigen-based detection of SARS-CoV-2 using nanomechanical sensor platform

Dilip Kumar Agarwal [a], Vikas Nandwana [a], Stephen E. Henrich [b], Vara Prasad V.N. Josyula [c], C. Shad Thaxton [b], Chao Qi [d], Lacy M. Simons [e,f], Judd F. Hultquist [e,f], Egon A. Ozer [e,f], Gajendra S. Shekhawat [a,**], Vinayak P. Dravid [a,*]

[a] Department of Material Science and Engineering and NUANCE Center, Northwestern University, Evanston, IL, 60208, USA
[b] Department of Urology, Feinberg School of Medicine, Northwestern University, Chicago, IL, 60611, USA
[c] Cleveland Clinic, Lerner Research Institute, Cleveland, OH, 44195, USA
[d] Department of Pathology, Feinberg School of Medicine, Northwestern University, Chicago, IL, 60611, USA
[e] Department of Medicine, Division of Infectious Diseases, Northwestern University Feinberg School of Medicine, Chicago, IL, 60611, USA
[f] Center for Pathogen Genomics and Microbial Evolution, Institute for Global Health, Northwestern University Feinberg School of Medicine, Chicago, IL, 60611, USA

ARTICLE INFO

Keywords:
Microcantilever
SARS-CoV-2
Detection
Sensitivity
Antigens
Sensor

ABSTRACT

The rapid spread of COVID-19 including recent emergence of new variants with its extreme range of pathologies create an urgent need to develop a versatile sensor for a rapid, precise, and highly sensitive detection of SARS-CoV-2. Herein, we report a microcantilever-based optical detection of SARS-CoV-2 antigenic proteins in just few minutes with high specificity by employing fluidic-atomic force microscopy (f-AFM) mediated nanomechanical deflection method. The corresponding antibodies against the target antigens were first grafted on the gold-coated microcantilever surface pre-functionalized with EDC-NHS chemistry for a suitable antibody-antigen interaction. Rapid detection of SARS-CoV-2 nucleocapsid (N) and spike (S1) receptor binding domain (RBD) proteins was first demonstrated at a clinically relevant concentration down to 1 ng/mL (33 pM) by real-time monitoring of nanomechanical signal induced by antibody-antigen interaction. More importantly, we further show high specific detection of antigens with nasopharyngeal swab specimens from patients pre-determined with qRT-PCR. The results take less than 5 min (swab to signal $\leq$5 min) and exhibit high selectivity and analytical sensitivity (LoD: 100 copies/ ml; 0.71 ng/ml of N protein). These findings demonstrate potential for nanomechanical signal transduction towards rapid antigen detection for early screening of SARS-CoV-2 and its related mutants.

1. Introduction

The outbreak of Severe Acute Respiratory Syndrome Coronavirus-2 (SARS-CoV-2) has resulted in over 220 million cases worldwide including 4.56 million deaths, as of September 7, 2021. Given the long incubation period of COVID-19 (2–14 days) and its highly contagious nature, the early and large-scale screening of COVID-19 is of paramount importance to reduce viral transmission. Since the FDA EUA approved real-time qRT-PCR for molecular diagnosis of COVID-19, it has been utilized as a 'gold standard' for SARS-CoV-2 detection (World Health Organization, 2021). However, RT-PCR suffers from long turnaround time due to complicated sample preparation and laboratory analysis which affects the diagnostic accuracy (Tahamtan and Ardebili, 2020). In addition, the need for specialized instruments to perform the test and specialists to operate the equipment make it un-reachable in resource-poor settings. Immunoassays to detect SARS-CoV-2 antigens are an alternative to PCR-based testing approaches, and they offer significant potential benefits. There are antigen tests available, but they often suffer from higher false-positives and false-negatives rates (Scohy et al., 2020). The inaccurate tests are in fact detrimental to disease spread and its management. Hence, there continues to be an urgent need for a rapid, cost-effective, point-of-care (POC) antigen tests that can directly detect SARS-CoV-2 immunogenic proteins with high sensitivity and specificity even before the onset of symptoms.

Since the start of this pandemic, researchers have employed different methodologies for the detection of SARS-CoV-2 virus in conjugation

* Corresponding author
** Corresponding author ,
E-mail addresses: g-shekhawat@northwestern.edu (G.S. Shekhawat), v-dravid@northwestern.edu (V.P. Dravid).

https://doi.org/10.1016/j.bios.2021.113647
Received 28 July 2021; Received in revised form 7 September 2021; Accepted 13 September 2021
Available online 17 September 2021

with the standard qRT-PCR test. Researchers demonstrated fabrication of a graphene-based FET (Field-Effect Transistor) sensor for the rapid detection of SARS-CoV-2 after functionalizing it with antibody against SARS- CoV-2 spike protein (Seo et al., 2020). Saline gargle solution was used to detect SARS-CoV-2 nucleoprotein peptides in COVID-19 infected patients using Mass spectroscopy technique (Ihling et al., 2020). Researchers have also employed humanized antibody-based method for the colorimetric detection of SARS-CoV-2 nucleocapsid protein (Kasetsirikul et al., 2020). Thus, there is a continued need to develop sensing or diagnostic assays for Covid-19 disease based on multiple antigens associated with SARS-CoV-2 virus. Most lateral flow assays utilize nucleocapsid (N) protein which has not undergone significant mutational changes. The viral spike protein (S) in fact, has evolved in recent months through mutations and some variants may escape neutralizing antibodies from the vaccine (Zhang et al., 2020; Hahn et al., 2020). Therefore, there is an urgent unmet need for an antigen test that can be accurate (through multiplexing and with redundancies), fast (less than 5 min from swab to signal), POC (point-of-care), sensitive, and fulfils many other economic and ergonomic considerations.

Microcantilever-based sensor platforms have been used significantly over the decades in biomolecular detection due to their low cost, high sensitivity, rapid response, and label-free detection system (Agarwal et al., 2018, 2020; Larvik et al., 2004; Boisen et al., 2011). The microcantilever sensor platforms work as a transducer for the translation of a biomolecular recognition phenomenon on its surface into a deflection signal (Fritz et al., 2000). These microsensors are preferred since they consist of an integrated array inside a chip which makes them amenable for parallel detection of several analytes at a time (Tamayo, 2013). Herein, we demonstrate an ultra-rapid ($\leq$5 min), highly sensitive (LoD: 100 copies/ml; 0.71 ng/ml of N protein), high-specificity detection of SARS-CoV-2 in nasopharyngeal swab specimens from the patients that were cross corroborated with prior qRT-PCR method to establish commensurate proportion of the viral load (copies/ml). Prior to detection, corresponding antibodies were first coated on the gold coated cantilever surface using EDC-NHS chemistry (Singh et al., 2020; Viola et al., 2015; Samantha and Sarkar. 2011; Fischer, 2010). We initially optimized the assay by detecting SARS-CoV-2 major immunogenic spike (S1) and nucleocapsid (N) proteins by employing microcantilever sensor platform with a detection sensitivity down to 1 ng/ml (33 pM). Further, we successfully demonstrated the specificity of our developed sensor through cross-validation using MERS-CoV and Influenza A viral samples on the microcantilever surface. We also studied the binding efficacy of spike RBD protein from mutant U.K variant (Alpha/B.1.1.7) with respect to their wild-type counterpart on the microcantilever surface.

2. Materials and methods

2.1. Chemical reagents and materials

SARS-CoV-2 Chimeric monoclonal antibody for spike (S1) protein (40150-D003), SARS-CoV-2 Chimeric monoclonal antibody for nucleocapsid (N) protein (40588-R0004), SARS-CoV-2 spike (RBD) protein (40150-V08B2), SARS-CoV-2 nucleocapsid (N) protein (40588-V08B), and MERS-CoV nucleocapsid protein (40068-V08B) were all purchased from Sino Biological Inc. Recombinant Human coronavirus SARS-CoV-2 glycoprotein (ab281471) and FITC labelled-anti SARS-CoV-2 spike glycoprotein antibody (ab282742) were purchased from Abcam. Phosphate Buffer Saline (PBS), PBS-Tween 20 sachets, Bovine Serum Albumin (BSA), and 11-Mercaptoundecanoic acid (MUA) were purchased from Millipore-Sigma. 1-Ethyl-3-(3-dimethylaminopropyl) carbodiimide and Sulfo-NHS were received from ThermoFisher Scientific. Nasopharyngeal swab specimens were collected from individuals presenting to Northwestern Memorial Hospital, Chicago. The spike protein (S1-RBD) from mutant UK variant B.1.1.7 was also purchased from Sino Biological Inc (40591-V08H12). The set-up used for the deflection measurements was Bruker Bioscope Resolve liquid imaging system. The tipless silicon cantilevers used in these experiments were acquired from Nanoworld Incorporation.

2.2. Preparation and functionalization of the microcantilever surface

The gold coated cantilevers were plasma cleaned prior to antibody immobilization step to remove any organic residues. The anti-SARS-CoV-2 antibodies (against S1 and N proteins) were covalently attached onto the gold coated cantilever surface through EDC-NHS chemistry inside a glass plate containing tiny wells (See Supplementary Information, Fig. S3). First, the cantilevers were immersed in 10 mM solution of 11-Mercaptoundecanoic acid (MUA) prepared in Ethanol to graft carboxylic groups on the surface followed by rinsing multiple times through DI water. The activation of these carboxylic groups was carried out by putting the cantilevers for incubation in a 100 μl solution mixture of 5 mM Carbodiimide EDC and 5 mM Sulfo-NHS in DI water. After rinsing with DI water, these functionalized microcantilevers were incubated overnight at 4°C in 20 μg/ml of antibody solutions (separately against S and N proteins) prepared in PBS and 0.05% bovine serum albumin (pH 7.4) to facilitate the covalent immobilization (Fig. 2). Here bovine serum albumin (BSA) was used to block the remaining sensor surface to minimize non-specific interaction. We first performed multiple experiments to optimize the antibody coverage on the cantilever surface and chose 20 μg/ml as optimum concentration for the deflection measurements (see Supplementary Information, Fig. S1). Microcantilevers were finally washed with PBS-tween-20 solution, dried and then fixed in the AFM sample holder. The sensor characterization for antibody immobilization and antigen binding has been shown in Supplementary Information (Fig. S6).

2.3. Experimental detection method

Specific biomolecular binding results in lateral stress that imposes a bending moment on the free end of the microcantilever. The microcantilever bends upwards or downwards in response to a tensile or compressive surface stress, respectively. The deflection can be monitored real-time with exquisite sensitivity, similar to AFM in operation. The receptor-coated microcantilever is typically positioned next to a passivated reference cantilever for a differential signal read-out to improve specificity in the detection. The sensitivity in these measurements is governed by ability to measure minute slightest deflections quantitatively and reproducibly.

The tipless gold coated silicon cantilevers used in these experiments (500 μm long, 95 μm wide and 1 μm in thickness) were acquired from Nanoworld Incorporation (See Supplementary Information, Fig. S2). The cantilevers and experimental conditions used in each measurement were similar. The absolute deflection at the free end of each cantilever (Δz) was measured using a fluidic-atomic force microscopy (f-AFM) based optical detection system. The relation between the deflection signal and resultant differential surface stress $\Delta\sigma$, is expressed by the famous Stoney's equation (Stony, 1909),

$$\Delta\sigma = 1/4.(t/L)^2.E/(1-\nu).\ \Delta z$$

where L is the effective length of the cantilever, t is the thickness, and $E/(1-\nu)$ is the ratio between the Young's modulus E (130 GPa for Si) and Poisson ratio ν (0.28 for Si). The force constant of these cantilevers was around 0.03 N/m. Because a cantilever deflection also strongly depends on geometry, all the cantilevers used in these measurements were exactly similar in their geometry. The positive (upward) or negative (downward) cantilever bending due to change in surface stress as a result of antibody-antigen interaction is directly related to the quantitative measurements for the bindings. The deflection experiments were performed inside a microfluidic reaction chamber sized approximately 2 mm in diameter while maintaining a constant temperature. The biofunctionalized microcantilevers were brought in close proximity to a

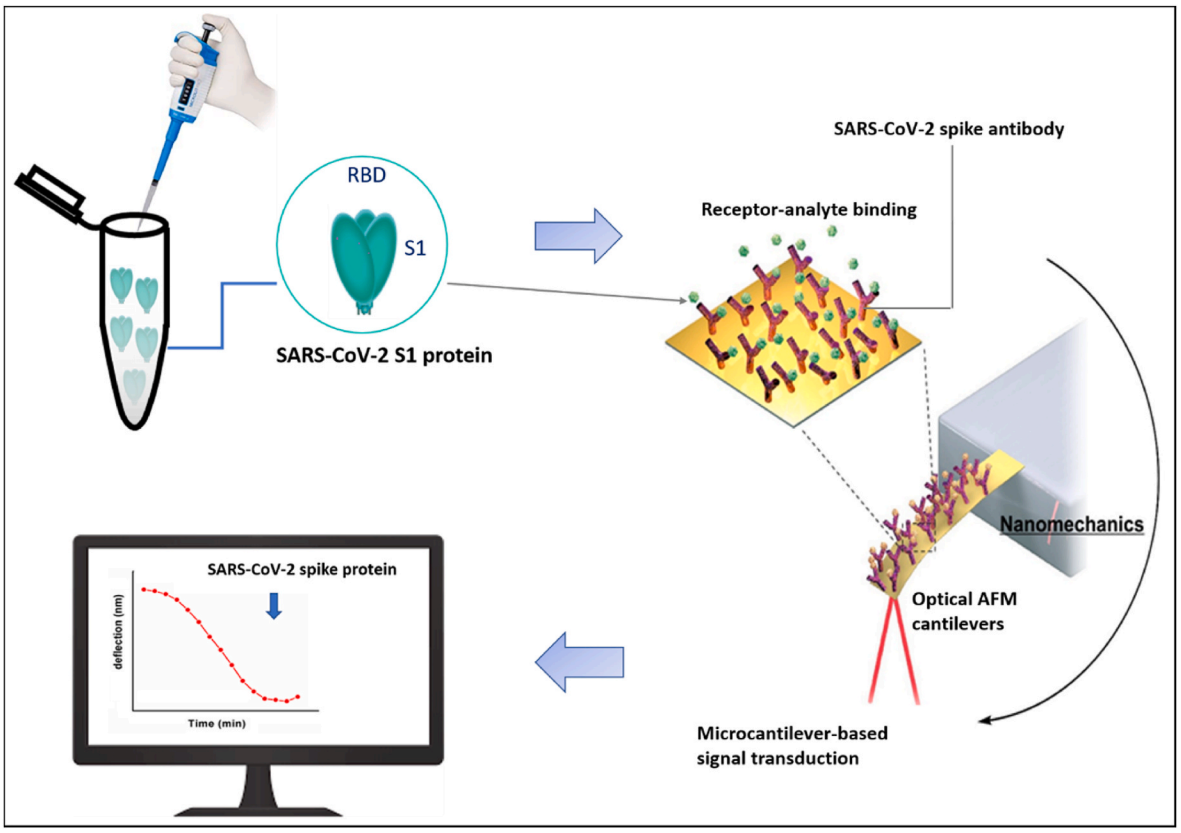

Fig. 1. Optical detection scheme for SARS-CoV-2 S1 (RBD-Receptor Binding Domain) protein on a microcantilever surface.

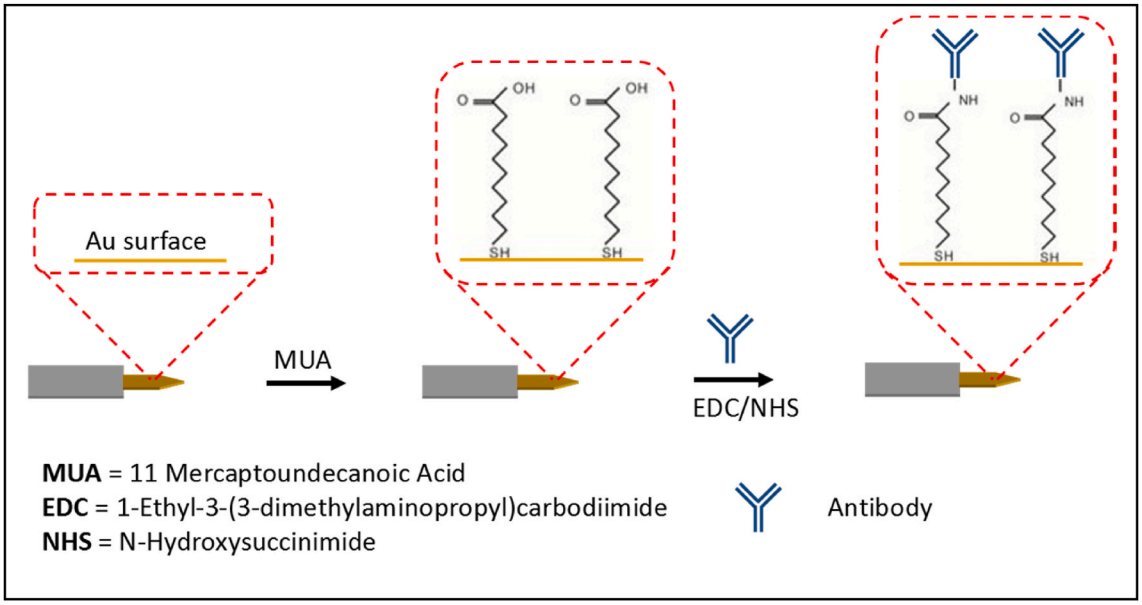

Fig. 2. Schematic of cantilever biofunctionalization using EDC-NHS chemistry. Monoclonal antibodies for spike and nucleocapsid proteins were immobilized on functionalized microcantilever surface.

microfluidic chamber containing antigen solution (10 μl approx) with the help of a stepper motor. The deflection experiments were performed for different concentrations of SARS-CoV-2 spike (S1) and nucleocapsid proteins (N) prepared in PBS buffer (pH 7.4); in addition to clinical patient samples. The magnitude of deflection was measured as cantilever start bending (downwards) due to differential surface stress.

3. Results and discussion

3.1. Detection of SARS-CoV-2 spike (S1) protein

The micro cantilever based optical detection system was first employed to detect SARS-CoV-2 S1 proteins. Apart from being a major transmembrane structural protein, spike protein is also highly

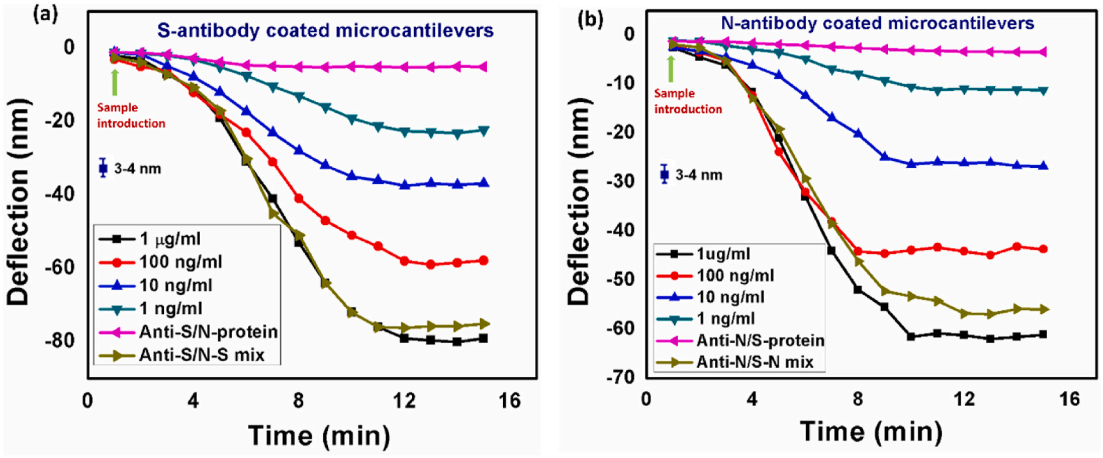

(c)

Target concentration	S1- protein deflection (nm) +/- 3-4 nm	N- protein deflection (nm)+/- 3-4 nm
1 μg/ml (3.3× 10^4 pM (S1)/ 2.1× 10^4 pM (N)	79.20	61.59
100 ng/ml (3.3× 10^3 pM (S1)/ 2.1× 10^3 pM (N)	58.23	44.56
10 ng/ml (3.3× 10^2 pM (S1)/ 2.1× 10^2 pM (N)	37.72	26.28
1 ng/ml (33.0 pM (S1)/ 21.0 pM (N)	22.10	11.76

Fig. 3. Concentration dependant response curves for SARS-CoV-2 S1 and N proteins; cross-validation and control experiments were also performed by interacting both S1 and N proteins in different combinations on the cantilever surface to ascertain the specificity in the detection, (a) Deflection plots for S1 protein detection, (b) Deflection plots for N protein, (c) Table for deflection values for different concentrations of S1 and N protein. Anti-S/N protein: detection of N protein onto anti-S1 antibody conjugated cantilever (cross-validation); Anti-S/N–S mix: interaction of N and S1 protein mixture solution onto an anti-S1 antibody coated cantilever surface (cross-validation); anti-N/S protein: detection of S1 protein onto anti-N antibody conjugated cantilever (cross-validation); anti-N/S–N mix: interaction of S1 and N protein mixture solution onto an anti-N antibody conjugated cantilever surface. The measurements were performed on multiple cantilevers for each concentration. Though, the data represented here is for individual cantilever to demonstrate our sensor characteristics.

immunogenic and possesses diverse amino acid sequences among the corona virus family making it an important target to develop a specific diagnostic platform for SARS-CoV-2 (Grant et al., 2020). Microcantilevers biofunctionalized with anti-S1 protein antibody (20 μg/ml) were used to quantify the detection signal using different concentrations of S1 protein (1 μg/ml, 100 ng/ml, 10 ng/ml, and 1.0 ng/ml, respectively). The real-time deflection measurement was monitored for 15 min, as demonstrated in Fig. 3a. We observed the deflection signal within 2–3 min of sample introduction which can be abbreviated to specific and selective interaction between the antibody and viral antigen on the cantilever surface. As shown in the figure, the sensor signal started saturating after 10–11 min of antibody-antigen reaction. The deflection signal (Δz) exhibited descending trends with decreasing antigen concentrations, i.e., 1 μg/ml (79.20 ± 3–4 nm), 100 ng/ml (58.20 ± 3–4 nm), 10 ng/ml (37.70 ± 3–4 nm), and 1 ng/ml (22.10 ± 3–4 nm), respectively, demonstrating highly specific binding between anti-S1 antibody and S1 protein. As illustrated in Fig. 3 (a), the cantilever with highest S1 concentration (1 μg/ml) showed a maximum bending signal (79.20 ± 3–4 nm) whereas cantilever with the lowest antigen concentration (1 ng/ml) showed the minimum response (22.10 ± 3–4 nm). These results can be attributed to the specific biomolecular interaction between the antibody and its corresponding target antigen resulting in an increased compressive stress on the cantilever surface, and thus generating a large deflection signal (Wu et al., 2001, 2013). The observed signal was reproducible with in ± 3–4 nm of variation for a given concentration after running series of experiments.

3.2. Detection of SARS-CoV-2 nucleocapsid (N) protein

After successfully demonstrating the S1 protein detection, we further investigated the cantilever response towards the SARS-CoV-2 nucleocapsid (N) protein. It is one of the 5 major non-structural proteins of coronavirus which is highly immunogenic and has more stable and conserved amino acid sequences among the coronaviruses (Lu et al., 2020). This intrigued us to study N protein mediated cantilever deflection and its comparison with S1 protein signal. Microcantilevers biofunctionalized with anti-N protein antibody (20 μg/ml) were used for the deflection measurements. As shown in Fig. 3b, the maximum cantilever deflection (61.59 ± 3–4 nm) was measured for 1 μg/ml of N-protein concentration, whereas the minimum cantilever deflection

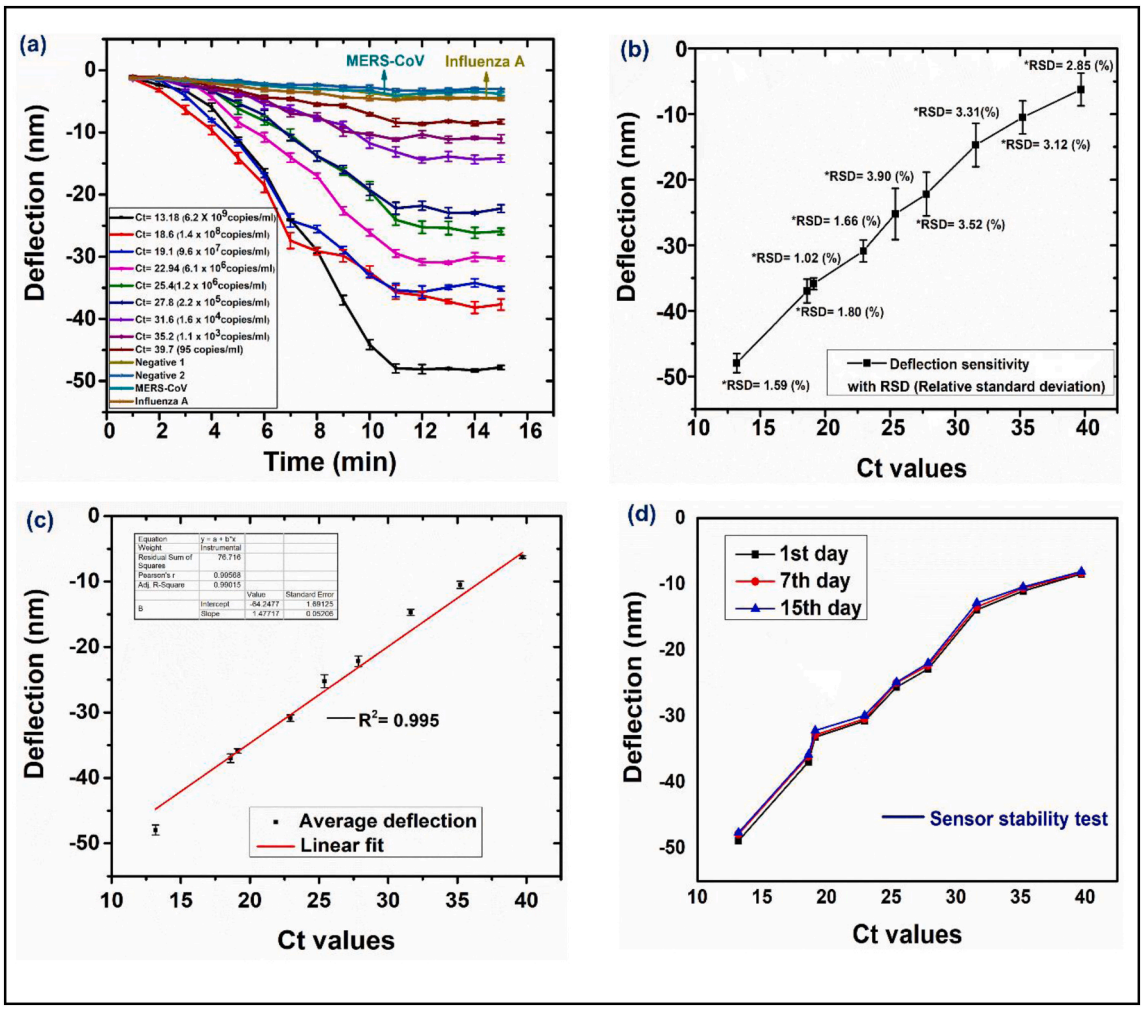

Fig. 4. Optical deflection measurement on patient samples with different Ct values. The curve represents deflection measurement for each Ct value along with the corresponding viral load (copies/ml) in the patient samples collected. The positive sample with the highest Ct value (39.7) yielded the lowest deflection (6.25 ± 3–4 nm) whereas maximum deflection (47.97 ± 3–4 nm) was exhibited for the patient sample having the lowest Ct value (13.18). The sensor did not show any measurable deflection for non-specific samples from MERS-CoV and Influenza A virus strain demonstrating specificity of the sensor, (b) Deflection curve for different Ct values with relative standard deviation (RSD) values. Error bars represent the standard error of three cantilevers, (c) Representation of deflection curve after the linear fitting, (d) Sensor stability measurement for a different period of time. The sensor exhibited stability in the data without losing any significant sensitivity for a period of fifteen days. The deflection and related RSD values have been provided in a tabulated form in Supplementary Information (Table S4).

(11.76 ± 3–4 nm) was exhibited by the lowest antigen concentration (1 ng/ml). Fig. 3 (a & b) shows that the observed values for cantilever deflection in the case of S1 protein was large in comparison with N protein for all the concentrations used which can be explained with the difference in the magnitude of surface stress generated in both the cases (Tamayo, 2013). The observed experimental variation in deflection between the measurements was found to be in the range of ± 3–4 nm and hence we have incorporated an error bar in each plot (Fig. 3 a and b).

Further, in order to establish the specificity and to greatly increase the efficacy of our detection method to specific markers, we performed some cross-validation experiments to check the cross-reactivity with N and S1 proteins in different combination (Surkova et al., 2020; Ramdas et al., 2020). First, the cantilever coated with anti-S1 antibody was allowed to react with SARS-CoV-2 N protein (1 μg/ml) and the data was recorded. Fig. 3a (pink line) shows that the cantilever did not show any significant deflection signal (approximately 3–4 nm) due to the absence of any specific antibody-antigen interaction on its surface after the introduction of N protein. Furthermore, another cantilever coated with anti-S1 antibody was allowed to interact with a mixture of N and S1 protein solution (Anti-S/N–S mix), using 1 μg/ml concentration for each protein. As seen in Fig. 3a (brown line), the deflection profile was found to be similar (76 ± 3–4 nm) to the detection curve for S1 protein alone (black line, Fig. 3a) indicating a specific interaction between anti-S1 antibody and S1 protein. Similar experiments were performed for anti-N antibody coated cantilevers (Fig. 3b) which were then interacted with S1 protein (pink line) and a mixture of N and S1 proteins (anti--N/S–N mix) in separate experiments. These cantilevers also demonstrated the similar trends with a maximum bending signal for N protein and a negligible deflection with the non-specific S1 protein. The experiments conducted here ascertain that our sensor platform is not only sensitive, but highly specific for SARS-CoV-2 spike and nucleocapsid protein detection. Fig. 1c displays the deflection values for S1 and N protein from the different optical measurements conducted for this study.

3.3. SARS-CoV-2 detection in clinical samples from COVID-19 patients

Having successfully detected S1 and N proteins in isolation, we then sought to demonstrate the sensitivity of our microcantilever system for detecting SARS-CoV-2 in patient specimens. The nasopharyngeal swabs samples were freshly collected from the patients admitted in the hospital

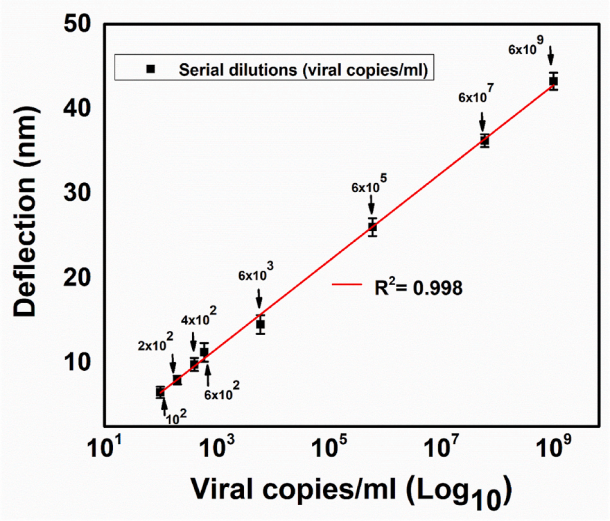

Fig. 5. Curve for serial dilution measurement of patient sample for the determination of LoD. A series of eight different dilutions were used from a SARS-CoV-2 positive specimen with a cycle threshold (Ct) value of 13.18 (6×10^9 copies/ml). The experiments were conducted on three individual microcantilevers. The error bar in the curve represents the standard error of the mean.

(Johnson, 1990). Prior to testing, the samples underwent a viral heat inactivation procedure by incubating in a water bath at 65°C for 30 min (Batejat et al., 2021; Burton et al., 2021). The positive samples used for the study had a spectrum of Ct values consistent with high (low Ct value) and low (high Ct value) viral load. The information regarding patient sample collection and processing has been placed in the Supplementary Information (SI). The deflection measurements were carried out with respect to the different Ct values from nine different patient samples. As seen in Fig. 4a, the positive sample with the highest Ct value (39.7)/(≈ 95 copies/ml) yielded the lowest deflection (6.25 ± 3–4 nm) whereas maximum deflection (47.97 ± 3–4 nm) was exhibited by the patient sample having the lowest Ct value, i.e. 13.18 (≈ 6.2×10^9 copies/ml). This is consistent with the fact that samples with the high Ct values generally have low viral load and hence low concentrations of N protein (≈ 0.71 ng/ml for the highest Ct value (39.71)-calculated from the standard N protein data) present in the solution to interact with the corresponding antibody on the cantilever surface as opposed to the sample with a low Ct value. As described earlier, more and high affinity binding events result in increase in the resultant stress on the cantilever surface causing more deflection. In addition, we further evaluated the deflection signal with samples collected from healthy subjects with no SARS-CoV-2 infection (negative samples). As shown in Fig. 4a (top navy blue and golden olive curves lines), there was no significant deflection for the samples taken from non-COVID individuals. This implies that there is very little or no nucleocapsid protein present in the sample to bind to its target antibody. We assert that despite limited number of samples, the data demonstrate potential practical and rapid (<5 min from swab to signal) detection of SARS-CoV-2 antigens in patient sample with high sensitivity, specificity, and selectivity. The different Ct values and viral load (viral copy numbers) along with their corresponding cantilever deflection $(Avg.)_{max}$ values from SARS-CoV-2 positive and negative individuals are given in Supplementary Information (Table S3). The detailed information regarding the viral copies number in all patient samples is given in Supplementary Information (Table S2).

Further, in order to demonstrate repeatability and reproducibility, the data were plotted with the relative standard deviation (RSD) for all the Ct values (Fig. 4b). The curve doesn't show much variation in the deflection sensitivity within each Ct value validating our detection method. Also, the sensor demonstrated a good linearity towards the virus detection ($R^2 = 0.995$), as seen from Fig. 4c. We then conducted a stability test to check the long-term storability of our sensor. Th cantilever devices were coated with antibody against the SARS-CoV-2 S1 protein and stored at 4°C till further use for target detection. As seen in Fig. 4d, the deflection sensitivity for a cantilever incubated for fifteen days remained almost the same as the 1st day sensitivity level (≈ 0.5–1.0 nm deflection decay). These results clearly suggest that our sensor is stable enough to be developed as a point-of-care platform for COVID-19 diagnostics.

3.4. Specificity of the sensor

The sensor devices were subjected to demonstrate that our sensor is highly specific to SARS-CoV-2 proteins only. Sensor specificity measurements were conducted by employing Influenza A (H1N1) and MERS-CoV virus sample, as represented in Fig. 3a. Nasopharyngeal swab samples collected from patients infected with Influenza A (H1N1) virus with a higher viral load (Ct = 19.33) was applied onto the cantilevers coated with SARS-CoV-2 nucleocapsid antibody. The result from this measurement revealed that the cantilever device did not show any measurable reactivity with H1N1 viral nucleocapsid protein. We then also evaluated sensor specificity using MERS-CoV nucleocapsid protein

Table 1
A comparison in sensor performance of reported and commercially available SARS-CoV-2 diagnostics with our microcantilever sensor platform (Zhena et al., 2020; fda, 2021).

Entity	Speed (time)	Sensitivity	Analytical sensitivity (LoD)	Attributes	References
SD Biosensor (Roche diagnostics)	15–30 min	99.2%	0.25–1.25 ng/ml	Antigen test (LFA)	Corman et al. (2021)
BinaxNOW™ COVID-19 Ag card (Abbott)	15 min	84.6%	4.04×10^4 copies/swab	Antigen test (LFA)	Frediani et al. (2021); Perchetti et al. (2021)
ID now COVID-19 (Abbott)	13 min	100%	20,000 copies/ml	Isothermal amplification (LAMP assay)	Basu et al. (2020)
XpertXpress SARS-CoV-2/Flu/RSV (Cepheid)	Not known	97.9%	100 copies/ml	qRT-PCR	Leung et al. (2021)
Simoa SARS-CoV-2 N protein antigen test (Quanterix)	2–3 h	97.7%	0.09 pg/ml	Antigen test (Sandwich ELISA)	Shan et al. (2021)
RIDA® SARS-CoV-2 rapid antigen test (R-Biopharm)	20 min	95%	237TCID50/ml	Antigen test (LFA)	Kohmer et al. (2021)
MIP-based N-antigen detection	15–20 min	Not known	27 fM	Electrochemical	Raziq et al. (2021)
Graphene based spike (S) antigen detection	5 min	Not known	100 fg/ml	Field Effect Transistor	Seo et al. (2020)
Cell based detection of spike antigen	3 min	92.8%	1-10 fg/ml	Electrochemical	Mavrikou et al. (2021)
***Microcantilever technology**	**≤ 3 min**	**98%**	**100 copies/ml (0.71 ng/ml of N protein concentration)**	**Antigen test (Nanomechanical)**	**This work**

sample prepared in PBS buffer solution. The measurement showed negligible deflection signal cross-validating our sensor specificity. These results confirm that our sensor is highly specific to SARS-CoV-2 and opens up substantial possibilities to be developed as a point-of-care platform for COVID prognosis and its management.

3.5. Evaluating limit of detection (LOD) through serial dilution

In order to determine the experimental limit of detection (LoD) of our developed sensor, eight serially diluted samples were prepared from the clinical patient sample corresponding to the reported highest Ct value, i.e. 13.18 (6.2×10^9 copies/ml). All the samples were incubated in the lysis buffer (extraction buffer) for some time before applying on the cantilever devices for optical deflection experiment (fluidic AFM). The plot in Fig. 5 indicates a strong linear relationship between the logarithms ($\log_{10}$) of viral concentrations from 100 copies/ml to 6×10^9 copies/ml and their corresponding deflection values ($R^2 = 0.998$). As seen in the plot, the highest deflection (44.25 nm) was observed for the undiluted sample with highest viral load (6×10^9 copies/ml) whereas the sample with the lowest viral load (100 copies/ml) demonstrated the minimal deflection (6.68 nm). The sensor was not able to detect viral copies in further dilutions (<100 copies/ml) which implies that the observed limit of detection (LoD) of our sensor can be considered as ≈100 viral copies/ml which is at par or better than many technologies reported in the literatures and currently available in the market (Zhena et al., 2020; fda, 2021). The deflection values of the patient sample with different serial dilutions have been shown in Supporting Information (Table S5).

3.6. A performance comparison with other existing platforms

Table 1 demonstrates a comparison between the different SARS-CoV-2 detection platforms reported in literature and currently in use and our developed platform with respect to its speed (time), sensitivity, specificity, and limit of detection (LoD). The sensor capabilities of our platform include its high speed of detection (swab to signal ≤ 5 min) making it high throughput, higher analytical sensitivity (low LOD), capable of detecting mutant strain, and a possible multiplexing with integrated electronics and sensor array. The lower limit of detection (100 copies/ml; 0.71 ng/ml) is crucial in COVID testing and its management when a very low viral load is present during the initial days of infection, and first sign of disease appears. For qRT-PCR based assay, any sample above a Ct value of 35 is considered as negative which is the range of sensitivity (LoD) for qPCR (Perchetti et al., 2021). The higher analytical sensitivity of our sensor can produce significantly lower false negative results which is very critical in pandemic control and can be a game changer in COVID diagnostics.

Since new SARS-CoV-2 variants are emerging rapidly (eg. newly emergent Delta variant), we further extended our study to find the binding affinity of spike protein (S1) from mutant U.K variant (B.1.1.7) with wild type antibodies from the original strain (Xie et al., 2021; Tang et al., 2021; Li et al., 2020; Jackson et al., 2021; Weng et al., 2021). We hope and anticipate such studies may further guide the development of therapeutics and vaccine against SARS-CoV-2 (Gomez et al., 2021). The detailed binding study of mutant UK variant on the cantilever surface has been provided in the Supplementary Information (Fig. S7 and Table S6).

4. Summary and conclusions

In this work, we demonstrated microcantilever-based nanomechanical detection of SARS-CoV-2 in patients' nasopharyngeal swab samples with high degree of sensitivity, specificity, and selectivity in just a few minutes ("swab to signal" in less than 5 min). The sensor exhibits an ultra-high level of sensitivity by detecting as low as 100 viral copies/ml (≈ 0.71 ng/ml of nucleocapsid protein) in patients' swab samples within a good linear range. The sensing capability of the developed platform was first determined by detecting SARS-CoV-2 S1 and N proteins at a concentration down to 1 ng/ml (33 pM). Patient sample data provided a favourable selectivity by showing no measurable deflection on samples from MERS-CoV and Influenza A virus, cross-validating our sensor platform. Our experimental results collectively demonstrate efficacy for a highly sensitive, and rapid antigen-based test for SARS-CoV-2 management and possess better sensor performance compared to reported and currently existing platforms. However, this technology lags in sensing multiple analytes at a time but our ongoing work on a possible multiplexing platform by integrating electronics and sensor arrays could pave a way for a rapid, accurate and cost-effective detection of COVID-19 antigens and potentially mutant variants together.

CRediT authorship contribution statement

Dilip Kumar Agarwal: Conceptualization, Methodology, Validation, Investigation, Data curation, Writing – original draft, Writing – review & editing, Visualization, Project administration. **Vikas Nandwana:** Methodology, Validation, Investigation, Data curation, Writing – original draft, Project administration. **Stephen E. Henrich:** Methodology, Validation, Resources, Writing – review & editing. **Vara Prasad V. N. Josyula:** Validation, Visualization, Writing – review & editing. **C. Shad Thaxton:** Validation, Resources, Writing – review & editing. **Chao Qi:** Resources, Validation. **Lacy M. Simons:** Resources, Validation. **Judd F. Hultquist:** Resources, Validation. **Egon A. Ozer:** Resources, Validation. **Gajendra S. Shekhawat:** Validation, Data curation, Investigation, Writing – original draft, Writing – review & editing, Visualization, Supervision, Project administration, Funding acquisition. **Vinayak P. Dravid:** Conceptualization, Validation, Data curation, Investigation, Writing – original draft, Writing – review & editing, Visualization, Supervision, Project administration, Funding acquisition.

Declaration of competing interest

The authors declare that they do not have any competing financial or personal interests which can influence the work reported in this paper.

Acknowledgement

This work made use of the SPID facilities of the NU*ANCE* Center at Northwestern University which has received support from Soft and Hybrid Nanotechnology Experimental (SH_yNE) Resource (NSF-ECCS-1542205), MRSEC program (NSF DMR-1121262) at the Materials Research Center; the International Institute for Nanotechnology (IIN); the Keck Foundation; and the State of Illinois, through the IIN. This work was supported by grant from the National Heart, Lung and Blood Institute Award Number 1400-SUB/3U54HL119810-07S1: Rapid Diagnostics of SARS-C0V-2 of Asymptomatic people returning to work and school.

Sample collection was supported by a COVID-19 pilot grant from the Northwestern University Clinical and Translational Science Institute (NUCATS, NIH grant UL1 TR001422); a Dixon Translational Research Grant made possible by the generous support of the Dixon Family Foundation; a CTSA supplement to NCATS UL1 TR002389; and a supplement to the Northwestern University Cancer Center P30 CA060553 (J.F.H., E.A.O.). Any opinions, findings, and conclusions or recommendations expressed in this material are those of the authors and do not necessarily reflect the views of the National Science Foundation and National Institutes of Health. Corresponding authors have intellectual property related to the diagnostic platform.

Appendix A. Supplementary data

Supplementary data to this article can be found online at https://doi.org/10.1016/j.bios.2021.113647.

References

Agarwal, D.K., Prasad, A., Vinchurkar, M., Gandhi, S., Prabhakar, D., Mukherji, M., Rao, V.R., 2018. Appl. Nanosci. 8, 1031–1042.

Agarwal, D.K., Kushagra, A., Ashwin, M., Shukla, A.S., Palaparthy, V., 2020. Nanotechnology 31, 115503.

Basu, A., Zinger, T., Inglima, K., Woo, K.-M., Atie, O., Yurasits, L., See, B., Rosenfeld, M. E.A., 2020. J. Clin. Microbiol. 8.

Batejat, C., Grassin, Q., Manuguerra, J.C., Leclercq, I., 2021. J. Biosaf. Biosec. 3, 1–3.

Boisen, A., Dohn, S., Keller, S.S., Maria, T., 2011. Rep. Prog. Phys. 74, 036101.

Burton, J., Love, H., Richards, K., Burton, C., Summers, C., Pitman, J., Easterbrook, L., Davies, K., Spencer, P., Killip, M., Cane, P., Bruce, C., Roberts, A.D.G., 2021. J. Virol Methods 290, 114087.

Corman, V.M., Haage, V.C., Bleicker, T., Schimdt, M.L., Mühlemann, B., 2021. Lancet 7, E311–e320.

fda, 2021. https://www.fda.gov/medical-devices/coronavirus-disease-2019-covid-19-emergency-use- authorizations-medical-devices/in-vitro-diagnostics-euas-antigen-diagnostic-tests-sars-cov-2 accessed 09-05.

Fischer, M.J., 2010. Methods Mol. Biol. 55–72.

Frediani, J.K., Levy, J.M., Rao, A., Basit, L., et al., 2021. Sci. Rep. 11, 14604.

Fritz, J., Baller, M.K., Lang, H.P., Rothuizen, H., Vettiger, P., Meyer, E., Guntherodt, H.-J., Gerber, C., Gimzewski, J.K., 2000. Science 5464, 316–318.

Gomez, C.E., Perdiguero, B., Esteben, M., 2021. Vaccine 9, 243.

Grant, O.C., Montgomery, D., Ito, K., Woods, R.J., 2020. Sci. Rep. 10, 14991.

Ihling, C., Tanzler, D., Hagemann, S., Kehlen, A., Hüttelmaier, S., Arlt, C., Sinz, A., 2020. J. Proteome Res. 19, 4389–4392.

Jackson, C.B., Zhang, L., Farzan, M., Choe, H., 2021. Biochem. Biophys. Res. Commun. 538, 108–115.

Jhonson, F.B., 1990. Clin. Microbiol. Rev. 3, 120–131.

Kasetsirikul, S., Umer, M., Soda, N., Sreejith, K.R., Shiddiky, M.J.A., Nguyen, N.T., 2020. Analyst 145, 7680.

Kohmer, N., Toptan, T., Pallas, C., Karaca, O., Pfeiffer, A., Westhaus, S., Widera, M., Berger, A., Hoehl, S., Kammel, M., Ciesek, S., Rabenau, H.F., 2021. J. Clin. Med. 10, 328.

Larvik, N.V., Sepenaik, M.J., Datskos, P.G., 2004. Rev. Sci. Instrum. 75, 2229.

Leung, E.C.-M., Chow, V.C.-Y., Lee, M.K.-P., Tang, K.P.-S., Li, D.K.-C., Lai, R.W.-M., 2021. J. Clin. Microl. 4.

Li, Q., Wu, J., Nie, J., Zhang, L., Zhao, H., Liu, S., Zhao, C., Zhang, Q., 2020. Cell 182, 1284–1294.

Lu, P.R., Zhao, X., Li, J., Niu, P., Yang, B., Wu, H., 2020. Lancet 10222, 565–574.

Mavrikou, S., Tsekauras, V., Hatziagapiou, K., Paradeisi, F., Bakakos, P., Michos, A., Koutsoukou, A., 2021. Bios 11, 224.

Perchetti, Garrett A., Greninger, Alexander L., 2021. Analytical sensitivity of the Abbott BinaxNOW COVID-19 Ag card. J. Clin. Microbiol. 59 (3), e02880–20. https://doi.org/10.1128/JCM.02880-20.

Ramdas, K., Darzi, A., Jain, S., 2020. Nat. Med. 26, 810–811.

Raziq, A., Kidakova, A., Boroznjak, R., Reut, J., Opik, A., Syritski, V., 2021. Biosens. Bioelectron. 178, 113029.

Samantha, D., Sarkar, A., 2011. Chem. Soc. Rev. 40, 2567–2592.

Scohy, A., Anantharajah, A., Bodéus, M., Mukadi, B.K., Verroken, A., Villalob, A.R., 2020. J. Clin. Virol. 129, 104455.

Seo, G., Lee, G., Kim, M.J., Baik, S.-H., Choi, M., Ku, K.B., 2020. ACS Nano 14, 5135–5142.

Shan, D., Johnson, J.M., Fernandes, S.C., , et al.Suib, H., Hawang, S., Wuelding, D., 2021. Nat. Commun. 12, 1931.

Singh, M., Kaur, N., Comini, M., 2020. J. Mater. Chem. 8, 3938—3955.

Stoney, G.G., 1909. Proc. Roy. Asoc. Lond. A 82, 172–175.

Surkova, E., Nikolayevskyy, V., Drobniewski, F., 2020. Lancet 8, 1167–1168.

Tahamtan, A., Ardebili, A., 2020. Expert Rev. Mol. Diagn. 5, 453–454.

Tamayo, J., 2013. Chem. Soc. Rev. 42, 1287–1311.

Tang, J.W., Tambyah, P.A., Hui, D.S.C., 2021. J. Infect. 82, e27–e28.

Viola, K.L., Sbarboro, J., Sureka, R., De, M., Bicca, M.A., Wang, J., Vasavada, S., 2015. Nat. Nanotechnol. 10, 91–98, 2015.

Wang, P., Nair, M.S., Liu, L., Iketani, S., Luo, Y., Guo, Y., Wang, M., Yu, J., 2021. Nature 593, 130–135.

who https://www.who.int/emergencies/diseases/novel-coronavirus-2019/technical guidance/ laboratory-guidance (accessed 09-05-2021).

Wu, G., Ji, H., Hansen, K., Thundat, T., Datar, R., Cote, R., Hagan, M.F., Chakraborty, A. K., Majumdar, A., 2001. Proc. Natl. Acad. Sci. Unit. States Am. 4, 1560–1564.

Wua, S., Nanb, T., Xuea, C., Chenga, T., Liuc, H., Wang, B., Zhang, Q., Wu, X., 2013. Biosens. Bioelctron. 48, 67–74.

Xie, X., Liu, Y., Liu, J., Zhang, X., Zou, J., Garfias, C.R.F., Xia, H., Swanson, K.A., Cutler, M., Cooper, D., 2021. Nat. Med. 27, 620–621.

Zhang, L., Jackson, C.B., Mou, H., Ojha, A., Peng, H., Quinlan, B.D., Rangarajan, E.S., Pan, A., Vanderheiden, A., 2020. Nat. Commun. 11, 6013, 2020.

Zhen, W., Smitha, E., Manjia, R., Schronb, D., Berry, G.J., 2020. J. Clin. Microbiol. 58, e00783, 20.